Temperature Dependence of Thermal Performance in Space Using Multilayer Insulation

Haruo Kawasaki, Shun Okazaki, Hiroyuki Sugita (JAXA)
Japan Aerospace Exploration Agency, Tsukuba-shi, Ibaraki-ken, 305-8505 JAPAN
and

Masahide Murakami (University of Tsukuba),

Graduate School of Systems and Information Engineering, University of Tsukuba,

1-1-1 Tennodai Tukubashi, Ibaraki 305-8573

Nomenclature

A	=	area, m^2	Subscripts		
C	=	constant	av	=	average temperature , K
d	=	diameter, m	B	=	boil-off tank or base plate
G	=	mass flow rate, $kg\ s^{-1}$	g	=	vapor
H	=	heat coefficient, $W\ m^{-2}K^{-1}$	Hem	=	hem of MLI blanket
h_L	=	latent heat of evaporation, $J\ kg^{-1}$	l	=	liquid
L	=	length, m	MLI	=	MLI outermost surface, Test MLI
N	=	number of MLI blanket, -	N	=	number of layers, number of test MLI
Q	=	amount of heat, W	n	=	number of control MLI blanket (masking MLI blanket)
q	=	heat flux, $W\ m^{-2}$			
T	=	temperature , K	S	=	outermost surface of MLI
t	=	thickness, m	$Total$	=	total into the boil-off tank, measured from evaporation rate by experiment
V	=	volume flow rate, $L\ min^{-1}$			
			V	=	vacuum chamber

Greek Letters

ε = emissivity, -

σ = Stefan-Boltzmann constant, $W\ m^{-2}K^{-4}$

ρ = density, $kg\ m^{-3}$

I. Introduction

Multilayer insulation (MLI) blankets are used for spacevehicles and satellites as excellent thermal control elements. The thermal performance (effective emittance) of MLI blankets has been measured by using the boil-off calorimeter method with liquid nitrogen (LN2) method capable of measuring the thermal performance of MLI blankets with a high degree of accuracy.

The effects of MLI blanket processing on the performance for space use have been measured by using the LN2 boil-off calorimeter method. And the effect of seams on the thermal performance of MLI blankets was found to be of principal importance. The heat loss from seams amounts to 50 %, with 23 % conduction, 18 % overlap, radiation of 10% between the layers, and a very small contribution from perforations. The best method of improving thermal performance is reducing the seam length and the conduction between layers.

We were not able to investigate the temperature dependences of the heat loss and the thermal performance of MLI blankets in our previous study. The temperature dependences, however, are important for the future spacevehicle design such as the moon exploration etc. The seams and hem of MLI blankets are effects on the thermal performance. The temperature effects of the seams and hem has not been obviously in the previous study.

In order to estimate the effects of temperature on the thermal performance of MLI, various working fluids were initially estimated for use with the boil-off calorimeter. The thermal performance of MLI blankets was then

1
American Institute of Aeronautics and Astronautics

measured by using the boil-off calorimeter method with another working fluid.   The temperature effect of seams and hem of MLI blankets on the thermal performance will be especially revealed in this study.

II.   Experiment with the boil-off calorimeter

A. Typical boil-off calorimeter

  Boil-off calorimeter measurement has often been used for measuring the thermal performance of an MLI blanket with high accuracy.

The experimental set-up for thermal performance measurement based on the calorimeter method with LN2 consists of a boil-off calorimeter, a vacuum pump, vacuum gauge, wet-type gas meter, data logger, water chiller and manometer.

Our boil-off calorimeter for use with LN2 was designed and produced in 2006. Our boil-off calorimeter used to measure thermal performance is shown in Figure 1. It is composed of three cylindrical LN2 tanks arranged vertically and a cylindrical outer shell. The three tanks are called the guard tank, boil-off tank and lower guard tank as viewed from above. The guard tank, boil-off tank and lower guard tank have volumes of 16.3 L, 19.8 L and 15.5 L, respectively. The boil-off tank that is the measurement tank has a cylindrical surface area of 0.2826 m^2. The outer shell, being a vacuum chamber, is also used as a thermal shield against the surroundings. The inner surface of the vacuum chamber is kept constant by controlling the water temperature in the jacket. The outer surfaces of the LN2 tanks are coated with black paint, and the inner surface of the vacuum chamber was treated with an anodic oxidation coating. The total hemispherical emissivity of the outer surfaces of the LN2 tanks and that of the inner surface of the vacuum chamber are 0.90 and 0.91, respectively.

Table 1 Specifications for the boil-off calorimeter with LN2

Component	Size or Specifications	note
Boil-off Tank	ϕ 0.3 m, height 0.3 m	Outer-surface: Black paint (Black Z306 polyurethane paint)
Guard Tank / Lower guard Tank	ϕ 0.3 m, height 0.24 / ϕ 0.3 m, height 0.23	Outer-surface: Black paint (Black Z306 polyurethane paint)
Vacuum Chamber	ϕ 0.6 m, height 1.3 m	Inside: Black anodize Aluminum, Water Jacket Pressure < 1.33×10^{-3} Pa
Gas flow meter	0.5 L/min	Wet-type
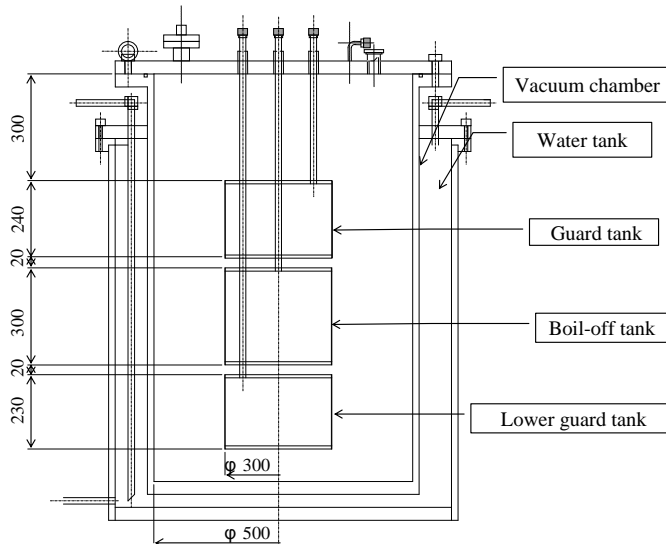
Figure 1 Schematic sketch of the boil-off calorimeter
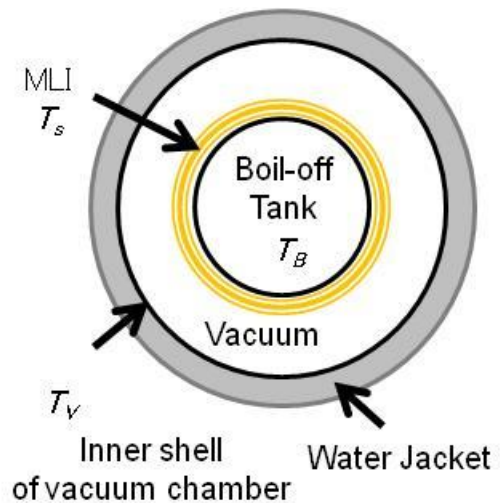
Figure 2 MLI in the boil-off calorimeter

The temperature of the boil-off tank of the calorimeter with LN2 was fixed at 77 K. To measure the temperature dependence of thermal performance in space using multilayer insulation, the temperature range of new boil-off calorimeter was considered.

B. Selection of working fluid

The temperature range and gas flow meter that we selected affected the working fluid of the boil-off calorimeter. The gas flow meter is important for measuring the net heat flow through the MLI blankets on the boil-off tank. The following equation was used to calculate the heat flow (Q_{total}) from the evaporation mass flow rate of the the working fluid G [kg s^{-1}] from the boil-off tank.

$$Q_{Total} = \frac{1}{1 - \frac{\rho_g}{\rho_l}} h_L G \tag{1}$$

The net heat flow through the MLI blankets can be expressed with effective emittance. The following equation defines the effective emittance that represents the thermal performance of an MLI blanket by using the MLI surface temperature (T_S) and base temperature (T_B).

$$\varepsilon_{eff} = \frac{q_{MLI}}{\sigma\left(T_S^4 - T_B^4\right)} \tag{2}$$

The use of surface temperature T_S, here is not suitable because it is not uniform in the MLI. However, effective emittance can be written with the uniform vacuum chamber temperature (T_V), as shown in eq.(3).

$$\varepsilon_{eff} = \frac{\varepsilon_s q_{MLI}}{\sigma\left(T_V^4 - T_B^4\right) - q_{MLI}} \tag{3}$$

The net heat flow (Q_{total}) through the MLI blankets was expressed with the effective emittance and sidewall area of the boil-off tank as shown in eq.(4).

$$Q_{Total} = \frac{\varepsilon_{eff}}{(\varepsilon_s + \varepsilon_{eff})} \sigma A\left(T_V^4 - T_B^4\right) \tag{4}$$

Various working fluids were estimated using eq.(1) and (4). According to this estimation, the effective emittance of MLI was supposed to be 0.01, and side-wall area of the boil-off tank was supposed to be 0.2826 m^2 the same as the area of our developed LN2 boil-off tank. Table 2 lists the results of our working fluid estimation. The evaporation volume flow rate (V) [L min^{-1}] can be calculated from the evaporation mass flow rate (G) [kg s^{-1}] . Given the high evaporation volume rate of helium, it is easy to measure its flow evaporation rate. Helium is already being used for in the low temperature range of a boil-off calorimeter, however, and entails the necessary handling of helium facilities. Moderate amounts of ethane and ammonia are also found in the evaporation rate and temperature range, but both are difficult to handle in terms of combustibility or toxicity. However, moderate amounts of Hydro Fluoro Carbon (HFC-134a) and Hydro Chloro Fluoro Carbon (HCFC-124) are also found in the evaporation rate and temperature range, and both are easy to handle for low combustibility and low toxicity. We selected HFC-134a because it is easier to obtain than HCFC-124.

Table 2 Candidates working fluids for the boil-off calorimeter

T_H [K]	T_B [K]	ε_{eff} [-]	q [W/m^2]	Q [W]	Working Fluid	V [L/min]	note
300	261	0.01	1.96	0.554	HCFC-124	0.0329	
300	247	0.01	2.48	0.702	HFC-134a	0.0426	
300	240	0.01	2.71	0.767	NH$_3$	0.0442	Toxicity
300	185	0.01	3.92	1.11	Ethane	0.1015	Combustibility
300	88	0.01	4.55	1.29	Argon	0.270	
300	77	0.01	4.57	1.29	N$_2$	0.314	Common fluid
300	4	0.01	4.59	1.298	He	21.42	

The evaporation volume flow rate of HFC-134a is one-tenth the flow rate of N_2. The boil-off tank for HFC-134a was made larger than that of the developed calorimeter for LN2 as listed in Table 2, in order to maintain reliability using the same gas flow meter as use for the developed calorimeter for LN2. Because HFC-134a is a global warming substance, the atmosphere release of HFC-134a is restricted. The boil-off calorimeter with HFC-134a forms a closed loop system to prevent any leakage of HFC-134ainto the atmosphere as shown in Fig.3. The boil-off calorimeter with HFC-134a consisted of the following three areas: a boil-off area, gas holder area and condensation area. The boil-off calorimeter area is the main part of the boil-off calorimeter and the same component of the LN2 calorimeter.

The gas holder area consisted of two gas holders, a gas flow meter and a pressure gauge. A bladder type gas holder was used to regulate atmosphere in the boil-off tank. The pressure gauge was used to check the gas holder pressure. The difference between the gas holder pressure and atmospheric pressure is less than 1kPa.

The condensation area consisted of a condenser/compressor, liquid HFC-134a cylinder and high pressure hose. Moreover, the condenser/compressor employed a commercial refrigerant recovery system (Recover XLT)

Table 3 Specifications of the boil-off calorimeter with HFC-134a

Component	Size or Specifications	note
Boil-off Tank	ϕ 0.3 m, height 450 m	Outer-surface: Black anodize Aluminum
Guard Tank /	ϕ 0.3 m, height 210 m/	Outer-surface: Black anodize Aluminum
Lower guard Tank	ϕ 0.3 m, height 150 m	
Vacuum Chamber	ϕ 0.6 m, height 1.3 m	Inside: Black anodize Aluminum, Water Jacket Pressure $< 1.33\times10^{-3}$ Pa
Gas flow meter	0.5 L/min	Wet-type
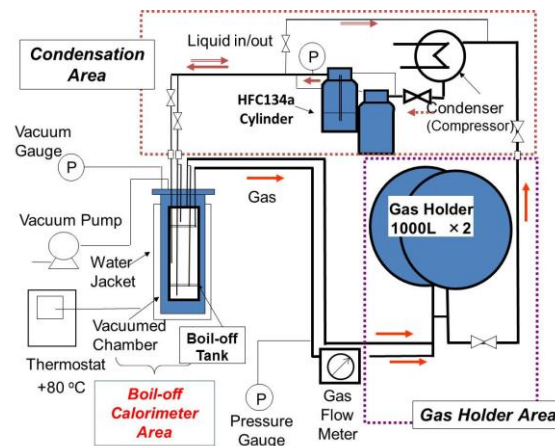
Figure 3 Schematic of the diagram of the boil-off calorimeter with HFC-134a
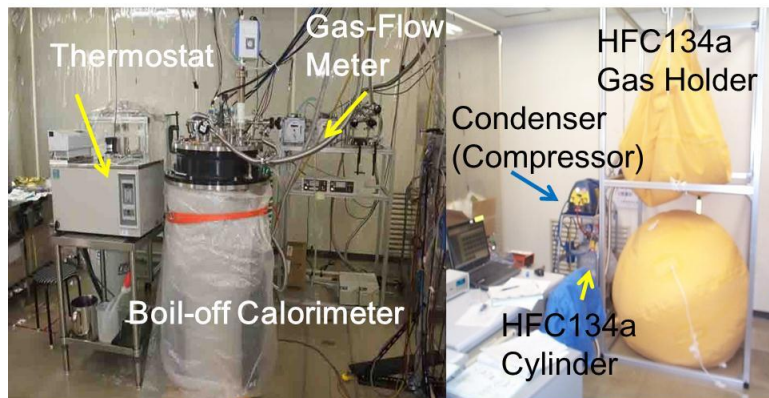
Figure 4 Photograph of boil-off calorimeter with HFC-134a
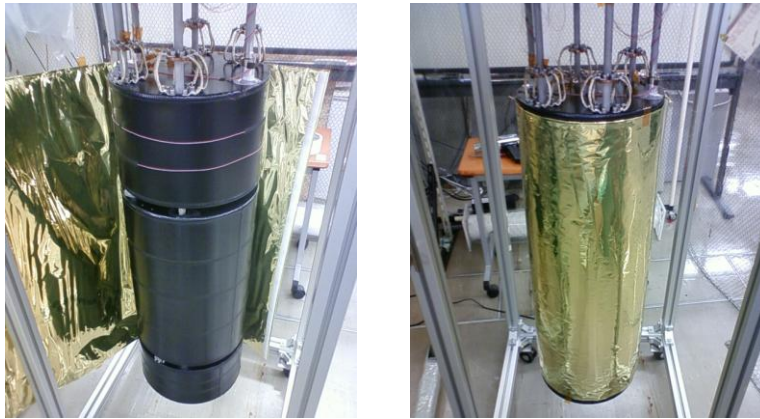
Figure 5 Photograph of the boil-off tank and guard tanks

C. Material properties of MLI

Table 4 lists data on the physical properties of films and nets used for MLI blankets as measured at room temperature. The emissivities of certain MLI materials and the boil-off calorimeter surface were measured at the room temperature by using a TESA2000 radiometer. The radiometer was used to measure all hemispherical emissivities of the black-painted part of the boil-off tank surface, the inner wall of the vacuum chamber, the aluminum-deposited side and polyimide side of polyimide films, and the aluminum-deposited polyester film.

Table 4 Material properties of MLI.

Material	Emissivity (normal)	Thickness, μm	Number of meshes, Meshes/cm^2
Polyimide film with aluminum vacuum-deposited on one side (polyimide surface)	0.68	24.9	-
Polyimide film with aluminum vacuum-deposited on one side (aluminum surface)	0.03	24.9	-
Polyester film with aluminum vacuum-deposited on both sides	0.03	6.4	-
polyester net	-	164	7.4

D. Test MLI blankets on boil-off calorimeter with HFC-134a

This experiment utilized commercially available MLI blanket that commonly often used for spacecrafts. It consists of a set of double-aluminized polyester films, polyester nets, and polyimide films of aluminum deposited only on one side. Each blanket is composed of 10 sets of alternately piled polyester film and polyester net, Table 5 below lists the composition in detail.

Framing needlework was performed along each hem of the MLI blankets with polyester thread at a stitching pitch of 3 mm to 7 mm. The hem stitching was done as loosely as possible by using a sewing machine. Adhesive thermal control tape having the same surface radiation characteristic as the outermost MLI blanket surface was used to prevent loosening of the hem of MLI blankets. The cross section of seam line zone of an MLI blankets is shown in Figures 6, 7. The hem region of each MLI blanket is more or less compressed by seam. Thermal control tape connects the outermost and the innermost layers. The locations of perforations in each layer are staggered from layer to layer with a diameter of 1 mm and a pitch of about 50 mm.

Table 5 Composition of MLI blanket examined in this study.

Layer number	Material
1(Outermost layer)	Polyimide film with aluminum deposited on one side (The polyimide side is made the face)
	≀
	polyester net
2∼11	polyester film with aluminum deposited on both sides
	≀
	polyester net
12(Innermost layer)	Polyimide film with aluminum deposited on one side (The polyimide side is made the face)
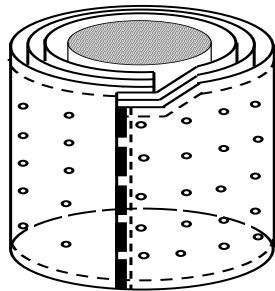
(a) MLI-D/10 : simple overlap   (b)   MLI-Non-processing   :
                                                     interleaved overlap
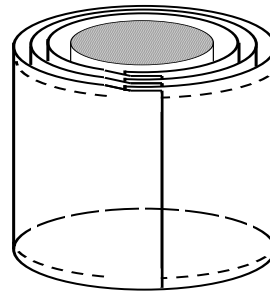
Figure 6 Configuration of MLI blankets
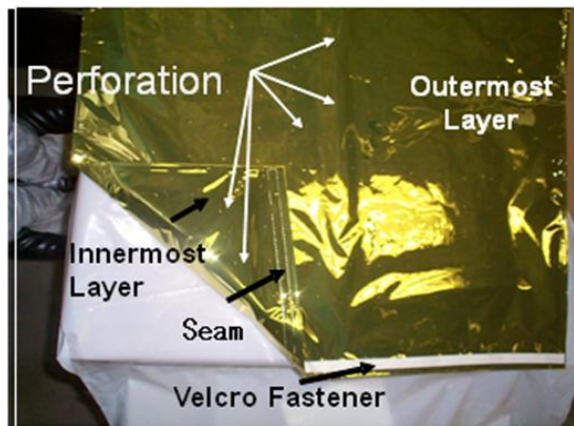
Figure 7   Processing of MLI blankets for space use

III.   Results and discussion of measurement by the boil-off calorimeter using HFC-134a

A. Measurement by the boil-off calorimeter using HFC-134a

MLI-D/10 was fixed on the boil-off tank and set up in the vacuum chamber. Liquid HFC-134a was transferred from the HFC-134a cylinder to the guard tank and boil-off tank, under pressure of 10^{-3} Pa in the vacuum chamber.

Temperature and HFC-134a flow rate in a steady state was shown in Figure 8. The temperature of the boil-off tank and inner wall of the vacuum chamber were 247.6 K and 321.7 K, respectively. The heat flow into the boil-off

American Institute of Aeronautics and Astronautics

tank was 1.16 W with heat flux 2.74W/m^2. The effective emissivity was 0.007 as using eq.(4). Table 6 lists the tests of MLI-D/10 and MLI-Non-processing. The heat leak from hem and velcro fastener Q_{Hem} of MLI-D/10 was 2.02 W/m which was estimated from the difference between the heat flow of MLI-D/10 and MLI-Non-processing.
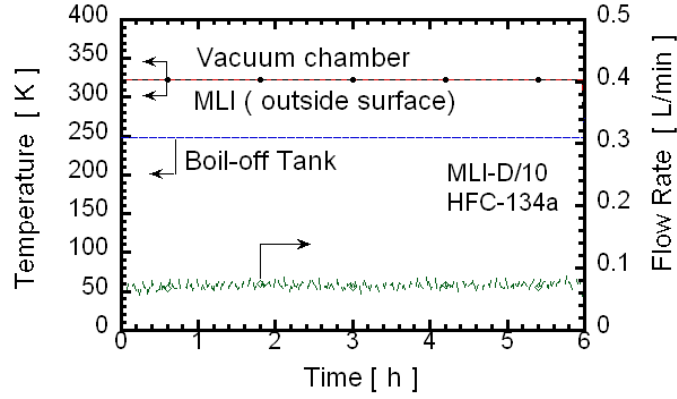
Figure 8 Time dependence of temperature and HFC-134a flow rate of the boil-off calorimeter with MLI-D/10

Table 6 Test results of changing the processing of MLI blankets

Name	Layer density [layer/mm]	Heat Flux [W/m^2]	Effective Emittance ε_{eff2} [-]
MLI-D/10	2.3	2.41	0.0061
MLI-Non-processing (MLI-Da(L2))	2.3	1.12	0.0028

B. Estimation of temperature dependence of MLI thermal performance

The LN2 boil-off calorimeter had already estimated thermal performances of MLI-D/10 and MLI-Non-processing. The effective emittance and heat transfer coefficient were arranged by average temperature as shown in Figures 9 and 10. The average temperature was defined as obtained in eq.(5).

$$T_{av} = \frac{T_V + T_B}{2} \tag{5}$$

And the heat transfer coefficient H_h [W/m^2 K] was defined as show in eq.(6).

$$H_h = \frac{q_{MLI}}{T_V - T_B} \tag{6}$$

An increase in the average temperature, reduced the effective emittance of MLI-D/10, and narrowed the variation in effective emittance of MLI-Non-processing as shown in Figure 9. Moreover, The heat transfer coefficient of MLI-D/10 and MLI-Non-processing were increased as shown in Figure 10.

C. Confirmation of temperature dependence of MLI thermal performance

The estimated data regarding the temperature dependence of thermal performance was confirmed based on the calculations and the data of previous work.

Heat flux between layers in MLI is calculated by eq.(7), assuming radiation flux is dominant in the MLI,

$$q_r = \frac{\sigma A_N}{\frac{1}{\varepsilon_{N+1}} + \frac{1}{\varepsilon_N} - 1} \left(T_{N+1}^4 - T_N^4 \right) \tag{7}$$

where N denotes the number of layers, q_r the radiation heat flux, σ the Stefan-Boltzmann constant, A_N the surface area, T_N the temperature of the N-th layer and ε_N is the emissivity of the layer. The temperature of the N-th layer

causes the emissivity of the layer to vary.. The temperature variation of the emissivity of aluminum was written in eq.(8).

$$\varepsilon_N = 1.63 \times 10^{-3} \times T^{0.495} \tag{8}$$

The heat flux of radiation-dominated MLI was calculated through the iterative calculation of Equations (7) and (8) for a set of initial trial values of the radiation heat flux and boundary temperature. The effective emittance and heat transfer coefficient were estimated from the calculated results of heat flux of the radiation-dominated MLI, as shown in Figures 9 and 10.

The effective emittance and heat transfer coefficient of MLI-Non-processing are slightly larger than the calculated effective emittance and heat transfer coefficient of radiation-dominated MLI. However, the effective emittance and the heat transfer coefficient of MLI-Non-processing and the calculation of radiation-dominated MLI show the same tendency.
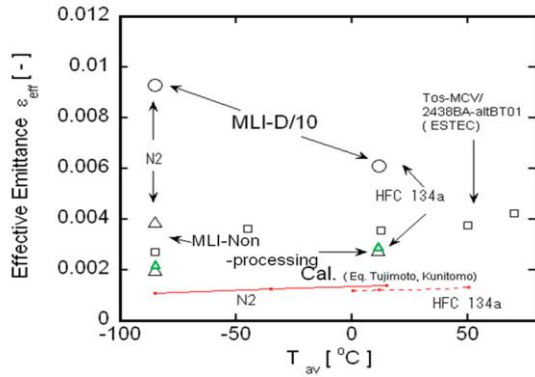
Figure 9 Relationship between average temperature and effective emittance.
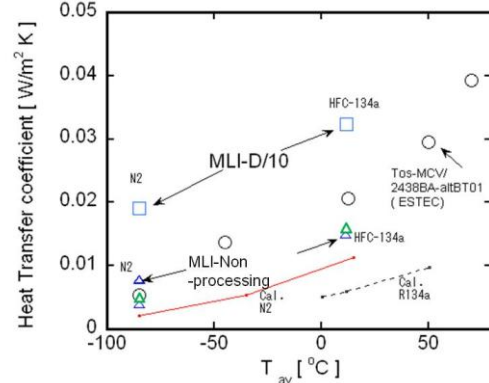
Figure 10 Relationship between average temperature and heat transfer coefficient.

The data of previous works[2] was plotted in Figures 9 and 10. The effective emittance and heat transfer coefficient of MLI-Non-processing and those obtained in previous work on MLI show the same tendency. Our boil-off calorimeter can thus be confirmed.

D. Analysis of temperature dependence of MLI-D/10

The effective emittance and heat transfer coefficient of MLI-D/10 are larger than those of MLI-Non-processing, due to heat flow from the processed parts of MLI-D/10. The heat flow ratio of MLI-D/10 was already analyzed using the LN2 boil-off calorimeter as shown in Figure 11. The heat flow from such processed part on MLI-D/10 such as hem was depended on the heat conduction in the MLI blanket. The heat flow of MLI-D/10 can thus be expressed by eq.(9) as follows:

$$Q_{MLI} = Q_R + Q_C + Q_{Hem}$$
$$Q_{MLI} = \varepsilon_{eff-R} \sigma A_{MLI} \left(T_V^4 - T_B^4 \right) + H_{MLI} A_{MLI} \left(T_V - T_B \right) + C_{Hem} L \left(T_V - T_B \right) \tag{9}$$

where Q_R can be estimated from eq.(7) , Q_C is estimated from thermal coefficient of the conduction between layers of MLI and Q_{Hem} is heat leak from hem. Q_{Hem} is consisted of heat leak at seam/ patch and simple overlap.

The average heat flux of MLI-D/10 is obtained as shown in eq.(10)

$$q_{MLI} = \varepsilon_{eff-R} \sigma \left(T_V^4 - T_B^4 \right) + \frac{\left(H_{MLI} A_{MLI} + C_{Hem} L \right)}{A_{MLI}} \left(T_V - T_B \right) \tag{10}$$

The thermal performance of MLI-D/10 with T_V: 323 K, T_B: 247 K (HFC-134a temperature range)and L:0.45 m was estimated from eq.(9) with constant H_{MLI} : 0.0044W/m²K and constant C_{Hem} : 0.012 W/mK which is estimated experimental MLI-D/10data at T_V: 300 K , T_B :77 K (LN2 temperature range). and ε_{eff-R} is 0.012.

Figure 12 shows the calculated effective emittance of MLI-D/10 as calculated by eqs. (10) and (2). The result of calculations and that our experiment were same tendency with average temperature. But the result value of

calculations was slightly lower than that of our experiment as shown in Figure 12. The calculated heat flow ratio in MLI-D/10 was shown in Figure 13. It was found that with increase in average temperature, effects of radiation in MLI-D/10 was relatively increasing.

   The heat flow ratio in MLI-D/10 estimated from experiment was shown in Figure 14. With the comparison of calculations and experiment at HFC-134a temperature range (Figure 13 and Figure 14) , the depends on the conduction, seam and patch and simple overlap in experiment were heavier than that of calculation.
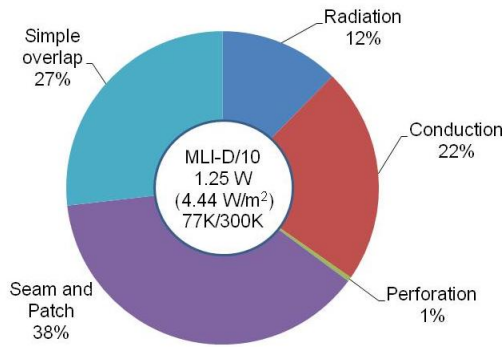
Figure 11 The heat flow ratio of MLI-D/10[1]
estimated from experiment with LN2
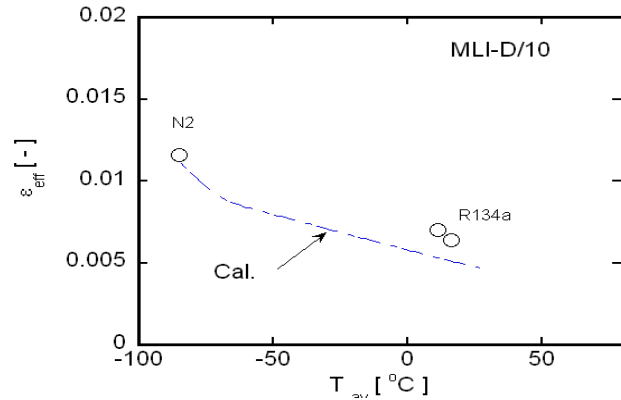
Figure 12 Comparison between calculations and
experimental effective emittance of MLI-D/10.
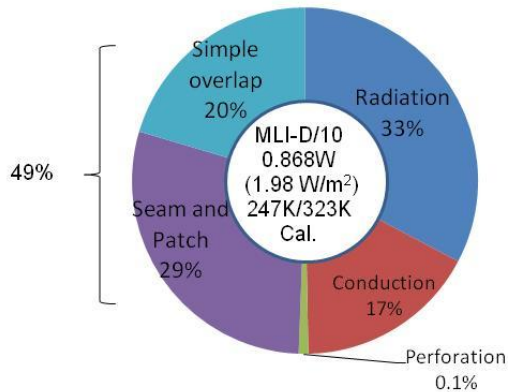
Figure 13 The heat flow ratio in MLI-D/10
calculated from eq.(9)
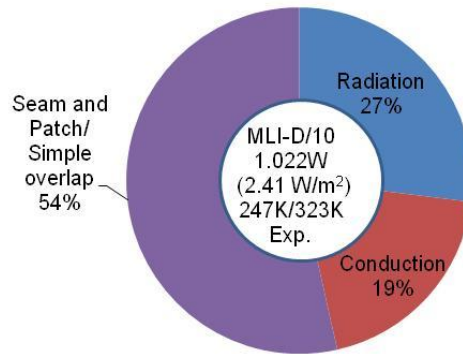
Figure 14 The heat flow ratio in MLI-D/10
estimated from experiment with HFC-134a

Temperature dependence of thermal constant and coefficient of MLI D/10 were rearranged in Table 7. It was found that the thermal constant at hem and coefficient of MLI are not constant and are increasing, with increase in average temperature. The change of the thermal constant and coefficient will be depended on thermal conductivity of MLI material.

Table 7 Temperature dependence of thermal constant and coefficient of MLI D/10

Temperature range	T_{av} [K]	$\varepsilon_{eff\text{-}R}$ [-]	H_{MLI} [W/m^{2}K]	C_{Hem} [W/mK]
77 K ~ 300K (LN2)	188.5 (-84.5 ^{o}C)	0.0012	0.0044	0.012
247K ~ 323 K (HFC-134a)	285 (12°C)	0.0017	0.0062	0.016

IV. Conclusion

In order to estimate the effects of temperature on the thermal performance of MLI blankets, candidate working fluids were considered for the boil-off calorimeter. We selected HFC-134a due to its low toxicity, low combustibility, evaporation temperature, and latent heat. The boil-off calorimeter method using HFC-134a was then designed and assembled. The boil-off calorimeter using HFC-134a forms a closed loop to prevent HFC-134a from being released into the atmosphere, as HFC-134a is a global warming substance.

The thermal performance of MLI blankets was measured by using the boil-off calorimeter method with HFC-134a. The effective emittance and heat transfer coefficient of MLI-Non-processing were slightly larger than the calculated effective emittance and heat transfer coefficient of radiation-dominated MLI. However, the effective emittance and heat transfer coefficient of MLI-Non-processing and the calculation for radiation-dominated MLI show the same tendency.

The effective emittance and heat transfer coefficient of MLI-Non-processing and the previous work done on MLI also show the same tendency. The thermal performance of MLI-D/10 at HFC-134a temperature range was calculated with experimental data of MLI-D/10 at LN2 temperature range. The result of calculations and that of our experiment were same tendency with average temperature. With increase in average temperature, effects of radiation in MLI-D/10 was relatively increasing. The result value of calculations was, however, slightly lower than that of our experiment.

By the comparison with calculations and experiment at HFC-134a temperature range, the dependence on the conduction, seam and patch and simple overlap in experiment were heavier than that of calculation. It was found that the thermal constant at hem and coefficient of MLI are not constant and are increasing, with increase in average temperature. The change of the thermal constant and coefficient will be depended on thermal conductivity of MLI material.

References

[1] Shun Okazaki, Masahide Murakami, Haruo Kawasaki, Takahiro Yabe, Hiroyuki Sugita and Yasurou Kanamori "Experimental study of the influence of processing on MLI performance for Space Use" 38th Int. Conference on Environmental Systems 2008-01-2067 (2008)

[2] R. Mayrhofer, I. Eberhart, C.Laa, C. Ranzenberger, A. Reissner, J. Stipsitz and B. Lehmann
" ESTEC Calorimeter: Thirty Five Years of Measurements" International Conference on Environmental Systems (ICES) 2009-01-2412 (2009)

[3] C. L. Tien and G. R. Cunnington, "Cryogenic Insulation Heat Transfer," Advances in Heat Transfer, Vol. 9, (1976)

[4] David G. Gilmore (ed.), Spacecraft Thermal Control Handbook Volume 1: Fundamental Technologies, 2nd ed., California, 2002, pp. 161-205.

[5] E. I. Lin, J. W. Stulz, and R. T. Reeve, "Test-derived Effective Emittance for Cassini MLI Blankets and Heat loss Characteristics in the Vicinity of Seams," AIAA parer, No. 95 - 2015, (June 1995)

[6] L. D. Stimpson and W. Jaworskis, "Effect of Overlaps, Stitches, and Patches on MLI," AIAA paper, No. 72 - 285, (1972)

[7] Jochen Doenecke, "Survey and Evaluation of MLI Heat Transfer measurement," SAE technical paper series, No.932117, (1993)

[8] E. M. W. Leung, R. W. Fast, H. L. Hart, and J. R. Heim, "Techniques for Reducing Radiation Heat Transfer Between 77 and 4.2 K", Advances in Cryogenic Engineering, Vol. 25, p489-p499, (1980)

[9] S. Jacob, S. Kasthurirengan and R. Karunanithi, "Investigations into the thermal performance of multilayer insulation (300-70 K) Part 1: Calorimetric studies, Cryogenics, 1992, Vol 32, No 12, p1137-1145

[10] M. P. Hnilicka, "Engineering Aspects of Heat Transfer in Multilayer Reflective Insulation and Performance of NRC Insulation," Advances in Cryogenic Engineering, Vol. 5 p199 - 208, (1960)

[11] G. R. Cunnington and C. L. Tien, "A Study of Heat Transfer Process in Multilayer Insulations," AIAA paper, No. 69 - 607, (1969)